Atmospheric fate and impact of perfluorinated butanone and pentanone

Yangang Ren, François Bernard, Véronique Daële, Abdelwahid Mellouki*

Affiliations

Institut de Combustion Aérothermique, Réactivité et Environnement, Centre National de la Recherche Scientifique (ICARE-CNRS), Observatoire des Sciences de l'Univers en région Centre (OSUC), CS 50060, 45071 cedex02, Orléans, France

Corresponding author

* mellouki@cnrs-orleans.fr

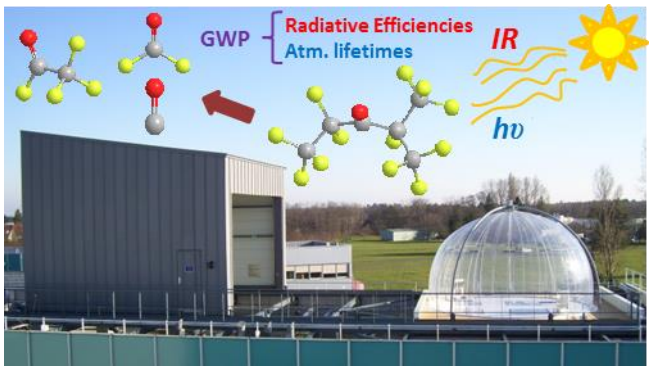
Journal: Environmental Science and Technology

Abstract

Perfluoroketones, used as replacement to halons and CFCs, are excluded from the Montreal Protocol because they are considered as non-ozone depleting substances. However, their chemical structure makes them possible greenhouse gases if their atmospheric lifetimes are long enough. To assess that possibility, we investigated the photolysis of perfluoro-2-methyl-3-pentanone (PF-2M3P), and perfluoro-3-methyl-2-butanone (PF-3M2B) using outdoor atmospheric simulation chambers. In addition, the photolysis of a non fluorinated pentanone (2-methyl-3-pentanone, 2M3P) was studied. The results showed that photolysis is the dominant loss pathway of PF-2M3P and PF-3M2B in the troposphere whereas 2M3P is lost by both photolysis and gas phase reaction with atmospheric oxidants. The photolysis effective quantum yields of PF-2M3P, PF-3M2B and 2M3P were estimated and some of the main products identified. The photolysis of PF-2M3P and PF-3M2B was found to have a minor impact on the atmospheric burden of fluorinated acids. The atmospheric lifetimes of PF-2M3P, PF-3M2B and 2M3P were estimated to 3-11 days, ~13 days and 1-2 days, respectively. Combining the obtained data, it has been concluded that with 100-year time horizon global warming potentials (GWP_{100}) equivalent to <0.21, ~0.29 and $\leq 1.3\times10^{-7}$ for PF-2M3P, PF-3M2B and 2M3P, respectively, these compounds will have a negligible impact on global warming.

Keywords: perfluorinated ketones, UV absorption spectrum, IR absorption spectrum, photolysis rates, natural irradiation, atmospheric lifetime, global warming potential.

TOC art



1. Introduction

Along with hydrofluorocarbons (HFCs), perfluorocarbons (PFCs) are non-ozone depleting substances and therefore excluded from the Montreal Protocol.[1] However, they are considered as greenhouse gases due to their strong absorption in the infrared spectral region in the atmospheric window combined to their long atmospheric lifetimes.[2] Their atmospheric concentrations have been growing rapidly over last decades and potentially continue to grow.[3] They have been widely used for the cooling of power electronics over the last decade. Perfluoroketones such as perfluoro-2-methyl-3-pentanone (PF-2M3P, $C_2F_5C(O)CF(CF_3)_2$, Novec 649/1230) and perfluoro-3-methyl-2-butanone (PF-3M2B, $C_2F_5C(O)CF(CF_3)_2$, Novec5110) are among the important replacement chemicals to halons and CFCs [4-5]. PF-2M3P and PF-3M2B are advanced heat transfer perfluorocarbons with high dielectric strength. Up to 30 t of PF-2M3P could be released into the atmosphere each year from fire-protection systems [6]. PF-3M2B is being used as versatile insulating gas for medium and high voltage applications including gas insulated lines, gas insulated switchgear and circuit breakers.[7] The large production and usage of both chemicals are likely to induce their direct emission into the atmosphere.

Similarly to other volatile organic compounds, PF-2M3P and PF-3M2B may be potentially removed from the atmosphere through photolysis, gas phase chemical reactions with the main atmospheric oxidants, hydrolysis and deposition. The

atmospheric fate of PF-2M3P has been subject to a limited number of investigations. Photolysis studies were based on the use of artificial and natural irradiations.[5,8,9] The atmospheric lifetime of PF-2M3P has been found to be controlled by photolysis and reported to be in the range of 4-14 days depending on latitude and period of the year.[6] The gas phase reactions with OH radical and ozone as well as hydrolysis represent minor contribution to the total removal of PF-2M3P from the atmosphere.[5-6] To the best of our knowledge, no experimental data on the photolysis of PF-3M2B have been reported. Hence, the present work aims at investigating the photolysis of PF-3M2B under atmospheric conditions and improving the existing data on PF-2M2B in order to evaluate their atmospheric impacts. In addition to the two perfluorinated ketones, a non-fluorinated analogue aliphatic ketone to PF-2M3P, 2-Methyl-3-pentanone (2M3P, $C_2H_5C(O)CH(CH_3)_2$) has been investigated. The UV-Visible and infrared (IR) absorption spectra of PF-2M3P, PF-3M2B and 2M3P were measured. Their photolysis rates were determined using two complementary atmospheric simulation chambers with natural sunlight irradiation. Atmospheric lifetimes and global warming potentials (GWP) for the three studied compounds are reported and discussed in terms of their atmospheric impacts.

2. Experimental Section

2.1. UV absorption spectra

The apparatus used in this work has been described in previous studies [8] and is briefly presented here. The UV-Visible absorption spectra of PF-2M3P, PF-3M2B, and 2M3P were measured using a spectrophotometer equipped with a 1200 grooves mm^{-1} grating and a charge-coupled device (CCD) camera. The collimated output of a 30 W deuterium lamp passed through a 100 cm long and 2.5 cm diameter Pyrex absorption cell equipped with quartz windows and focused onto the entrance slit of the spectrometer. Measurements were made over the wavelength region 220–400 nm by recording typically three overlapping regions of about 15 nm. Typically, each measurement consisted of 8-13 scans of diode array. The wavelength scale was calibrated using the emission lines from a low-pressure Hg pen ray lamps (253.7, 313.2, and 365 nm). Absorption cross sections, $\sigma(\lambda)$ (in cm^2 $molecule^{-1}$) were obtained using the Beer's law:

$$\sigma(\lambda) = \frac{-ln[I(\lambda)/I_0(\lambda)]}{CL} \qquad \text{Eq. 1}$$

where *L* is the path length of absorption cell (in cm), and *C* is the concentration of the studied compound (in molecule cm^{-3}). $I_0(\lambda)$ and $I(\lambda)$ are the light intensities in the absence and in the presence of the compound in the absorption cell, respectively. The concentration of the species of interest in the absorption cell was obtained from the measured pressure using a 0-10 Torr capacitance manometer. Measurements of the PF-2M3P, PF-3M2B and 2M3P UV absorption spectra were performed at T = (292±1) K using the concentration ranges [PF-2M3P] = (0.29 - 2.7) × 10^{17}, [PF-3M2B] = (0.27 – 3.0) × 10^{17} and [2M3P] = (0.43 – 2.9) × 10^{17} molecule cm^{-3}.

2.2. Atmospheric simulation chambers

Photolysis studies of PF-2M3P, PF-3M2B and 2M3P were conducted in the large simulation chamber HELIOS. In addition, the photolysis of PF-2M3P was also investigated in a 3.4 m^3 Teflon outdoor chamber. Both HELIOS and the 3.4 m^3 Teflon outdoor chambers allowed photolysis experiments to be performed under natural solar exposure.

2.2.1. HELIOS

The facility consists of a 90 m^3 hemispherical outdoor simulation chamber (47°50'18.39N; 1°56'40.03E) made of FEP Teflon film. This facility has been described previously.[9] The light transmission ranges from 88 to 95% over the entire solar spectrum. Two fans installed in the chamber ensure a rapid mixing of reactants (within less than 90 seconds). Solar actinic flux (290-660 nm) and photolysis frequencies of H_2O_2, HONO, HCHO, NO_3, NO_2 and $O(^1D)$ were measured by a spectroradiometer (Meteorologie Consult GmbH 6007). Pressure, relative humidity and temperature were continuously monitored by a three-axis Ultrasonic Anemometer (Delta Ohm, HD 2003) installed in the center of the chamber. The temperature distribution was also measured using six thermocouples (PT-100) spatially and equally distributed inside the chamber. A mobile protective housing kept the chamber under the dark and can be easily moved to fully expose the chamber to sunlight within 30

seconds. The experimental duration under irradiation was between 3 and 7 hours, in which the temperature typically increased by ~10 °C. Between experiments, the chamber was cleaned by flushing pure air through for at least 12 hours.

Organic compounds were monitored via in situ Fourier transform infrared spectrometry (FT-IR, Bruker Vertex70 spectrometer) coupled to a White-type multipass cell (302.6 m optical path length). Infrared spectra were recorded every 3 minutes by co-adding 250 interferograms with a resolution of 0.4 cm^{-1}. The gas phase mixture was also analyzed using a gas chromatography coupled to a mass spectrometer (GC-MS, PekinElmer Clarus 600 C). Gas samples were collected from the chamber at low temperature (-30°C) onto Air Toxics tubes and analyzed through a thermal desorber (TurboMatrix™ 150 ATD), with split mode, followed by a thermal desorption at 300 °C (5 min) delivering the sample to a 60-m column (GasPro diameter 0.320mm). The O_3 and NO-NO_x concentrations were continuously monitored by UV absorption (HORIBA, APOA 370) and chemiluminescence analyzer (HORIBA, APNA 360), respectively. PF-3M2B was also monitored by PTR-TOF-MS (Proton Transfer Reaction - Time of Flight-Mass Spectrometer, IONICON 8000). The fragment CF_3^+ (*m/z* 68.986) and $(CF_3)_2CF_3^+$ (*m/z* 168.970) were used to monitor the temporal behavior of PF-3M2B during the photolysis.

PF-2M3P and 2M3P were introduced into the chamber by placing known volumes of liquid in a bubbler and then, flushed by purified air. Their concentrations were derived based on the volume of the liquid introduced, the pressure and the temperature

in the chamber using the ideal gas law. PF-3M2B and SF_6 were introduced into the chamber by streaming purified air through a calibrated stainless steel cylinder (4.87 L) equipped with capacitance manometers. To compensate sampling flows from analytical instruments and chamber leaks, a flow of purified air (15-25 L/min) was added continuously during all experiments enabling a slight overpressure to be maintained, thus avoiding any contamination from outside air. Dilution of the gas volume in the chamber was determined by monitoring the decay of introduced amount of SF_6 (monitored by FT-IR). This decay under dark conditions was found to be in the range of $(5 – 20) \times 10^{-6}$ s^{-1}.

Background concentrations in the chamber were systematically found to be below the detection limits of analytical instruments (e.g., $[NO_x]<2.5\times10^{10}$, $[O_3]<2.5\times10^{10}$, [VOC] $<1.3\times10^{8}$ molecule cm^{-3}).

2.2.2. 3.4 m^3 outdoor chamber

Photolysis studies of PF-2M3P were also performed in the 3.4 m^3 ICARE outdoor atmospheric simulation chamber made of ethylene tetrafluoroethylene (ETFE) foil. The light intensity was continuously monitored using a filter radiometer measuring the photolysis frequency of NO_2, J_{NO2} (Meteorologie consult Gmbh, Germany). The temperature and the relative humidity were also continuously measured using a combined probe (Vaisala HMT330 series transmitters). Chemical analysis of the gas mixture was characterized by an infrared spectrometer (Nicolet 550 Magna FT-IR

spectrometer) coupled to a White-type multi-pass mirror cell (optical path length 10 meters). Infrared spectra were recorded every 5 minutes by co-adding 130 interferograms at a resolution of 1 cm^{-1}. Rapid mixing of reactant was insured using a fan made of Teflon mounted into the chamber. The dilution rate was estimated by monitoring the loss of SF_6. IR reference spectrum of PF-2M3P was obtained by introducing a known volume of liquid in the chamber. During dark experiments, the chamber was covered by a black and opaque curtain to protect it from sunlight radiation. The curtain could be removed very quickly for exposure to solar radiation, thus initiating the photolysis process. Experiments were performed at 1013 mbar of purified air and in the temperature range of 306 to 319 K. Initial concentrations of PF-2M3P were in the range of (0.89-2.7) × 10^{14} molecule cm^{-3}. The gas mixture was exposed to solar irradiation for up to 4 hours.

2.3. Photolysis experiments

Under sunlight conditions, the investigated ketones, PF-2M3P, PF-3M2B and 2M3P may be removed by photolysis, dilution and wall loss processes following the reactions:

ketones + $h\upsilon$ → products J (1)

ketones → dilution and wall loss k_L (2)

SF_6 → dilution k_d (3)

where J (in s^{-1}) is their photolysis rate while k_L (in s^{-1}) is their decay rates under the dark including dilution and wall loss. Under irradiation, the total decays of the investigated ketones are expressed as follows:

$$ln([ketone]_0/[ketone]_t) = k_{tot} \times t \quad \text{Eq. 2}$$

with $[ketone]_0$ and $[ketone]_t$ are the concentrations of PF-2M3P or PF-3M2B or 2M3P at times t_0 and t, respectively. k_{tot} (in s^{-1}), the total decay rate of the studied compound under irradiation, is formulated as:

$$k_{tot} = J_{meas} + k_{d,light} + (k_L - k_{d,dark}) \quad \text{Eq. 3}$$

J_{meas} is the photolysis rate obtained from the experiment measurement. $k_{d,dark}$ and $k_{d,light}$ (in s^{-1}) are, respectively, the dilution decay rates obtained from SF_6 decay in the dark and during irradiation.

The atmospheric photolysis rate coefficient was calculated, J_{calc}, as follows:

$$J_{calc} = \int \sigma(\lambda)\Phi(\lambda)F(\lambda)d\lambda \quad (\lambda = 290\text{-}400 \text{ nm}) \quad \text{Eq. 4}$$

where $\sigma(\lambda)$, $\Phi(\lambda)$ and $F(\lambda)$ are the absorption cross-section, the quantum yield of dissociation and the actinic flux over the absorption 290 to 400 nm, respectively. The actinic flux was directly measured by the spectroradiometer placed inside the chamber. Assuming a quantum yield of unity for the photodissociation process along the absorption region of PF-2M3P or PF-3M2B or 2M3P, the maximum photolytic rate coefficient can be calculated, $J_{max} = J_{cal}$ using Eq. 4. As a result, an effective photodissociation quantum yield can derived:

$$\Phi_{eff} = J_{meas}/J_{max} \quad \text{Eq. 5}$$

2.4. Chamber loss correction

The concentrations of the products formed from the photolysis of PF-2M3P, PF-3M2B and 2M3P were corrected to account for dilution and possible photolysis/OH reactions under irradiation using the following equation:[10]

$$[\text{Product}]_{corrected} = [\text{Product}]_{measured} \times F \quad \text{Eq. 6}$$

with F being the correction factor: $F = 1 + \Delta[\text{Product}]/ [\text{Product}]_{measured}$

The amount of product lost, Δ[Product] due to secondary reactions, i.e., dilution, reaction with OH radical and photolysis processes is calculated from:

$$\Delta[\text{Product}] = \int(k_{d,light} + J_{product} + [OH]^*k) \times [\text{Product}]_{measured} \times dt \quad \text{Eq. 7}$$

The losses of CF_3COF, COF_2 and CO were only due to dilution and were corrected using $F < 1.2$. For HCHO, CH_3CHO and CH_3COCH_3, photolysis, reaction with OH radical and dilution were considered and $F_{HCHO} < 1.52$, $F_{CH3CHO} < 1.35$ and $F_{CH3COCH3} < 1.30$ were used for the corresponding corrections. J_{HCHO} measured by the spectoradiometer and J_{CH3CHO} and $J_{CH3COCH3}$ were calculated using Eq. 4; corresponding σ(λ) and Φ(λ) values for CH_3CHO and CH_3COCH_3 were taken from IUPAC database[11]. The OH rate coefficients of CO, HCHO, CH_3CHO and CH_3COCH_3 were extracted from IUPAC kinetic database [11] as 1.65×10^{-13}, 8.5×10^{-12}, 1.5×10^{-11} and 1.8×10^{-13} cm^3 $molecule^{-1}$ s^{-1} at T = 298 K.

227

228 **2.5 Infrared absorption spectra**

229 The spectra of PF-2M3P, PF-3M2B, and 2M3P were measured at 295±1 K using
230 Fourier transform infrared (FTIR) spectroscopy. Absorption spectra were recorded in
231 250 co-adds between 700 and 4000 cm^{-1} at 1 cm^{-1} resolution (Happ-Genzel apodization).
232 A Whyte-type multi-pass absorption cell with 10 meters optical path length (KBr
233 windows) was used in the course of these measurements. Absorption spectra, $A(\upsilon)$
234 (base e), (or integrated band strengths) were determined using Beer's law:

235 $$A(\upsilon) = \sigma(\upsilon) \times L \times [\text{Ketones}] \qquad \text{Eq. 8}$$

236 where $\sigma(\upsilon)$ is the infrared absorption cross section of the ketones at wavenumber ν, L
237 is the absorption path length, and [ketones] is the PF-2M3P, PF-3M2B, and 2M3P
238 concentration. Measurements were performed using the following concentration ranges
239 (in units of molecule cm^{-3}): (1.2-10.8) $\times 10^{14}$ for PF-2M3P, (1.6-9.9)$\times 10^{14}$ for PF-3M2B
240 and (0.6-4.8) $\times 10^{14}$ for 2M3P. Over the course of the study, replicate measurements
241 were performed using independently prepared gas mixtures with helium as bath gas.
242 The absorption spectra (band strengths) were obtained from a linear least-squares fit of
243 A versus [Ketones] that included at least 6 individual spectrum measurements.

244

245 **2.6. Chemicals**

246 The chemicals used in this work and their stated purities were as follows:
247 perfluoro-2-methyl-3-pentanone (99%, 3M Belgium N.V, Chemical Group-EBC), 2-

methyl-3-pentanone (97%, Sigma-Aldrich), perfluoro-3-methyl-2-buytanone (98%, Ugarit Chimie), SF_6 (99.9995%, Air Liquide) and O_2 (99.9995%, Air Liquide), Helium (99.9995%, Air Liquide). PF-2M3P, PF-3M2B and 2M3P samples were further purified by using several freeze-pump-thaw cycles. GC-MS analysis of the samples did not show any observable impurities.

3. Results and Discussion

3.1. UV absorption cross section

To test the accuracy of the measurement methodology used in this work, the UV absorption spectrum of acetone has been measured and compared to the recommended UV spectrum from NASA/JPL evaluation.[12] As shown in SI (Figure S1), the level of agreement between both measured and recommended spectra is high, within the measurement accuracy of the recommended UV-Vis absorption spectra (≈8%). This excellent agreement provides confidence in the reliability of the absorption cross section measurement conducted in this work.

The measured UV-Visible absorption spectra of PF-2M3P, PF-3M2B and 2M3P between 220 and 400 nm at (300 ± 2) K are depicted in Figure 1 and absorption cross sections are provided in Table S1. The quoted uncertainties originated from 2 standard deviation (2σ) of the average of individual measurements. The measurements satisfied Beer's law over a wide concentration range (an order of magnitude). The measured absorbance, A (base e) ranged from 0.2 to 1.7 for PF-2M3P, 0.1 to 1.0 for PF-3M2B,

0.3 to 2.0 for 2M3P. Corresponding graphical representations of Beer's law fits are given in Figure S2.

2M3P shows a maximum absorption at 284 nm ($\sigma_{(284\ nm)}$ = (6.99 ± 0.28) × 10^{-20} cm^2 $molecule^{-1}$) while PF-2M3P shows a maximum around 305 nm ($\sigma_{(305\ nm)}$ = (6.50 ± 0.28) × 10^{-20} cm^2 $molecule^{-1}$) and PF-3M2B exhibits a maximum absorption at 300 nm ($\sigma_{(300\ nm)}$ = (3.46 ± 0.15) × 10^{-20} cm^2 $molecule^{-1}$). The UV absorption spectra obtained in this work are compared with those reported in literature when possible and are presented in Figure 1. The absorption spectrum of PF-2M3P is in agreement with the reported one by Taniguchi et al.,[5] within 5%. The absorption cross sections of 2M3P obtained in the present work is higher than that reported by Díaz-de-Mera, et al. [13] by 18% (σ_{max}). To the best of our knowledge, the experimental UV spectrum of PF-3M2B is reported for the first time here. Prior to this study, the UV spectrum of PF-3M2B was also determined using a theoretical approach and found to be higher compared to this work, within 27% at the maximum cross section.[14]

The absorption band of ketones is caused by the dipole forbidden n-π* transition of the C=O group. The maximum absorption of PF-2M3P is red-shifted, i.e. around 20 nm, compared to 2M3P caused by the electronegative substituents in α-α'-positions.[15-17] In addition, the maximum absorption of PF-2M3P is about ~2 times higher than that of PF-3M2B, which is consistent with the results of Mu and Mellouki [8] who observed that the peak UV cross section increased for larger aliphatic ketones.

The actinic flux in HELIOS at 13:00 (± 5 min, local time) on 7th of September

290 2013 is also displayed on Figure 1. The integrated absorption cross sections over the
291 actinic flux region for PF-2M3P, 2M3P and PF-3M2B were determined to be 2.61×10^{-18}, 1.22×10^{-18} and 1.25×10^{-18} cm^2 $molecule^{-1}$, respectively, indicating that one could
293 expect $J_{PF\text{-}2M3P} > J_{2M3P} \approx J_{PF\text{-}3M2B}$.
294
295 **3.2. Photolysis of perfluoro-2-methyl-3-pentanone**
296 **Photolysis rate measurements.** Experiments in the 3.4 m^3 outdoor chamber were
297 conducted in June-July 2010 at (306-319) K and RH<1%. Temporal profiles of PF-
298 2M3P and SF_6 concentrations were monitored under the dark for about 4 hours. No
299 discernible loss other than dilution has been observed; the first order decay rates of PF-
300 2M3P and SF_6 were in the order of $(6.6 - 8.1) \times 10^{-6}$ s^{-1}. The chamber was then exposed
301 to solar radiation, thus starting the photolysis. The photolysis rate of PF-2M3P, $J_{PF\text{-}2M3P}$,
302 was obtained by considering the total loss of PF-2M3P (k_{tot}) and that from dilution
303 which was obtained from the loss rate of SF_6 (k_d) under irradiation. Experimental details
304 and results derived from the four runs conducted are displayed in Table 1. For all
305 experiments, the photolysis rates of NO_2 were in the range of $(4.4\text{-}5.5)\times10^{-3}$ s^{-1}. The
306 consumed fractions of PF-2M3P from photodissociation were between 2.1 and 3.7 %
307 and the derived photolysis rates were $(1.7\text{-}2.8)\times10^{-6}$ s^{-1} under our experimental
308 conditions ($J_{NO2} = (4.4\text{-}5.5)\times10^{-3}$ s^{-1}). The quoted error corresponds to 2σ obtained from
309 the least square analysis applied on the experimental data. The estimated error on $J_{PF\text{-}2M3P}$ was in the range of 7-14 %.

HELIOS experiments were performed during September 2013 at T = 298 - 317 K and RH<1%. SF_6 and PF-2M3P concentrations were monitored by FT-IR and ATD-GC-MS for typically 2 hours in the dark and under natural irradiation for typically 4 to 7 hours. The loss rates of SF_6 and PF-2M3P were found to be similar in the dark, equivalent to $(4.8\text{-}6.0)\times10^{-6}$ s^{-1}, indicating a minor loss on the chamber wall of PF-2M3P. During irradiation, both FT-IR and ATD-GC-MS instruments showed a slightly higher disappearance rate of PF-2M3P than SF_6 which indicated a possible photolysis loss of PF-2M3P (ranging from 1.7 to 7.7 %) under our experimental conditions. The photolysis rate of PF-2M3P, $J_{PF\text{-}2M3P}$ was determined to be $(1.1\text{-}3.8)\times10^{-6}$ and $(1.1\text{-}3.6)\times10^{-6}$ s^{-1} using Eq. 3, from FTIR and GC-MS measurements, respectively, with a recommended range of $(1.1\text{-}3.8)\times10^{-6}$ s^{-1} (with $J_{NO2} = (3.0\text{-}5.6)\times10^{-3}$ s^{-1}).

Table 2 summarizes the photolysis rates of PF-2M3P obtained in this work and those reported in the literature. The values from this work were lower than those reported by D'Anna, et al. [18] Díaz-de-Mera, et al. [13] who also conducted experiments under natural irradiation in Spain. In contrast, the experiments conducted under artificial irradiation using black lamps or sunlamps led to lower photolysis rate values [5]. It should be noted that the measured photolysis rate from this work agreed with the result from the TUV model [19] run at different seasons of the year (Table S2).

The maximum photolysis rate of PF-2M3P, $J_{max\text{-}PF\text{-}2M3P}$, was estimated using absorption cross sections and the actinic flux measured in this work (Eq. 4) and found to be in the range of $(0.7\text{-}1.2)\times10^{-4}$ s^{-1}. Therefore, the observed photolysis rate

corresponds to an effective quantum yield of $\emptyset_{eff}$ =0.015-0.035, which is in agreement with the values reported by D'Anna, et al. [18] and Díaz-de-Mera, et al. [13], 0.043±0.011 and 0.044±0.006, respectively.

Products and mechanism. Typical IR spectra obtained from the photolysis of PF-2M3P/SF_6/air mixture in HELIOS are displayed in SI (Figure S3). CF_3COF, COF_2 and CO were identified as photolysis products by FTIR analysis from 3.4 m^3 chamber and HELIOS experiments. Perfluoro-propionic acid ($CF_3CF_2C(O)OH$, PFPrA) and trifluoro-acetic acid (CF_3COOH, TFA) were also identified (*m/z* 69) among the photolysis products, using the NIST GC-MS library (Figure S4). Temporal profiles of PF-2M3P and its photolysis products are depicted in Figure 2.

The formation yields of products (COF_2, CF_3COF and CO) were obtained from a linear least-square fit applied to the experimental data as shown in Figure S5 (HELIOS) and Figure S6 (3.4 m^3 chamber) and summarized in Table S3. The recommended formation yields of products (±2σ) from the photolysis of PF-2M3P are: (74±18)%, (193±84)%, and (204±68)% for $CF_3C(O)F$, COF_2, and CO, respectively. The carbon and fluorine budgets were estimated to (90±28)% and (57±18)%, respectively. This suggests a large fraction of unidentified fluorine-containing products. Indeed, Taniguchi, et al. [5] identified $CF_3O_3CF_3$ and CF_3OH as photolysis products that were not identified in the present work.

A proposed mechanism leading to the formation of the observed products from the photolysis of PF-2M3P is shown in Figure S7. The photodissociation of PF-2M3P may occur through a C-C bond cleavage in the α-position of the carbonyl group to produce perfluoroalkyl and perfluoroacetyl radicals:

$$CF_3CF_2C(O)CF(CF_3)_2 + h\upsilon \rightarrow CF_3CF_2 + C(O)CF(CF_3)_2 \quad (4)$$

$$\rightarrow CF_3CF_2C(O) + CF(CF_3)_2 \quad (5)$$

Perfluoroacetyl radicals are expected to either decompose to give CO and perfluoroalkyl radical:

$$(CF_3)_2CFC(O) \rightarrow (CF_3)_2CF + CO \quad (6)$$

$$CF_3CF_2C(O) \rightarrow CF_3CF_2 + CO \quad (7)$$

or react with O_2 leading to the corresponding peroxy radicals:

$$(CF_3)_2CFC(O) + O_2 + M \rightarrow (CF_3)_2CFC(O)O_2 \quad (8)$$

$$CF_3CF_2C(O) + O_2 + M \rightarrow CF_3CF_2C(O)O_2 + M \quad (9)$$

The high formation yield of CO (204±68)% indicates that the thermal decomposition is an important pathway in the fate of perfluoroacetyl radical over the reaction with O_2.

CF_3COF and COF_2, identified among the photolysis products (74±18)% and (193±84)%, respectively, might originate from the reactions of $CF_3CF_2O_2$ and $(CF_3)_2CFCO_2$ radicals with RO_2 radicals present in the system leading to the corresponding RO radicals as $(CF_3)_2CFCO$ and CF_3CF_2O radicals, which would

372 thermally decompose to form CF_3 radicals and the corresponding fluorinated carbonyls
373 $CF_3C(O)F$ and COF_2.[20] In addition, CF_3CF_2OH and CF_3OH, formed from CF_3CF_2O
374 and CF_3O radicals reaction with hydrogen-containing compounds present in the
375 chamber (e.g., HCHO desorbing from the chamber walls, impurities in the air diluent,
376 or water), were also reported to transform rapidly into COF_2.[21-22]
377
378 **3.3. Photolysis of 2-methyl-3-pentanone**
379 **Photolysis rate measurements**. Mixtures of 2M3P/SF_6/air were added into
380 HELIOS and left in the dark typically for 2 hours before irradiation by solar light. The
381 loss rates of SF_6 and 2M3P in the dark were determined to be (4.8-6.2) $\times 10^{-6}$ and (5.2-
382 6.8) $\times 10^{-6}$ s^{-1}, respectively. The chemical mixture 2M3P/SF_6/air was then exposed to
383 solar irradiation for typically 5-6 hours. Under these experimental conditions, the
384 measured loss of 2M3P ranged from 3.9 to 6.3%. The determination of J_{2M3P} from FTIR
385 and GC-MS measurements were in good agreement, within (3-7) %. The experimental
386 conditions and the obtained values of J_{2M3P} are summarized in Table 1.
387 All the experiments were performed in the absence of OH radical scavenger to
388 avoid spectral interferences in the mid-infrared region with the studied compounds.
389 Therefore, the gas phase removal of 2M3P during solar exposure might also due to the
390 reaction of OH radicals with 2M3P in addition to its photolysis. Indeed, when the
391 chamber was only filled with purified air and exposed to solar irradiation, separate
392 measurements using a chemical ionization mass spectrometer (CIMS) have shown the

393 presence of OH radicals at concentration ranging from $(2.1\pm0.9)\times10^5$ occasionally up
394 to 2×10^6 molecule cm^{-3} could be observed. This implied that under these conditions,
395 the OH reaction contribution to the total loss of 2M3P would have contributed from 30%
396 to 100%. However, it has been also observed that the disappearance rate of 2M3P
397 during solar exposure during this study was very comparable to those of PF-2M3P and
398 PF-3M2B (Table 1), suggesting that the OH concentration level during these
399 experiments was very low. Therefore, in the absence of OH radical direct measurement
400 during this study, we preferred to be conservative and thus, recommend an upper limit
401 for the photolysis rate of 2M3P, equivalent to $(2.6\pm1.4)\times10^{-6}$ s^{-1} (with $J_{NO2} = 5.6\times10^{-3}$
402 s^{-1}).

403 Based on the integrated UV absorption spectrum over the actinic flux region, the
404 derived maximum photolysis rate constant of 2M3P, $J_{max\text{-}2M3P}$, was found to be (6.5-
405 9.6)$\times10^{-6}$ s^{-1}. Therefore, the effective photolysis quantum yield is estimated to be $\emptyset_{eff}$
406 $=\leq0.28$ under tropospheric sunlight conditions.

407

408 **Products and mechanism.** Products were identified and quantified using FT-IR
409 spectroscopy. The Figure S8 displays the typical spectra acquired before and after the
410 photolysis of 2M3P. Comparison of measured calibrated IR spectra shows the presence
411 of CH_3CHO, CO, CH_3COCH_3 and HCHO among the oxidation products where an
412 example of time-concentration profiles of 2M3P and its products is shown in Figure S9.
413 These products have been observed to be of primary origin when 2M3P was exposed

to natural irradiation (Figure S10). As explained previously, derived formation yields of products, possibly accounted for both contributions of photolysis and OH reactions, were estimated to (81±18)%, (25±6)%, (90±16)% and (98±10)% for CH_3CHO, HCHO, CH_3COCH_3 and CO, respectively. Therefore, due to unquantified contribution of OH reaction to the formation yields of products during this photolysis study, we prefer to conclude qualitatively on the formation of CH_3CHO, HCHO, CH_3COCH_3 and CO among the photolysis products from the irradiation of 2M3P.

Figure S11 shows the proposed mechanistic pathways leading to the formation of the observed products. The photolysis of 2M3P may occur via C-C bond cleavage associated with C=O group to form an alkyl and the corresponding acetyl radical:

$$CH_3CH_2C(O)CH(CH_3)_2 + h\upsilon \rightarrow CH_3CH_2 + C(O)CH(CH_3)_2 \quad (10)$$

$$CH_3CH_2C(O)CH(CH_3)_2 + h\upsilon \rightarrow CH_3CH_2C(O) + CH(CH_3)_2 \quad (11)$$

$CH_3CH_2C(O)$ and $C(O)CH(CH_3)_2$ radicals, are expected to either decompose to alkyl radicals (CH_3CH_2 and $(CH_3)_2CH$) leading to CO elimination or react with O_2 to form the corresponding acetyl peroxy radicals ($(CH_3)_2CHC(O)O_2$ and $CH_3CH_2C(O)O_2$). CO formation indicating the occurrence of at least one of the decomposition channels 12 and 13:

$$(CH_3)_2CHC(O) \rightarrow (CH_3)_2CH + CO \quad (12)$$

$$CH_3CH_2C(O) \rightarrow CH_3CH_2 + CO \quad (13)$$

The reaction of $CH_3CH_2C(O)O_2$ with HO_2 radical has been reported to lead to the formation of $CH_3CH_2C(O)OH$ and O_3.[23] However, the absence of the carboxylic

435 acid and O_3 among the photolysis products indicates that the reaction of acetyl peroxy
436 radicals with HO_2 was insignificant under our experimental conditions. $CH_3CH_2C(O)O$
437 and $(CH_3)_2CHC(O)O$ radicals are expected to decompose to form the corresponding
438 alkyl radicals, CH_3CH_2 and $(CH_3)_2CH$, respectively.[23-24]

439 As shown in Figure S11, the subsequent reaction of CH_3CH_2 and $(CH_3)_2CH$ with
440 O_2 would form the corresponding peroxy radicals, $CH_3CH_2O_2$ and $(CH_3)_2CHO_2$. The
441 self-reaction of $CH_3CH_2O_2$ radical would lead to the formation of CH_3CH_2O radical
442 (60%) and CH_3CHO + CH_3CH_2OH (40%).[12] In addition, the $(CH_3)_2CHO_2$ radical self-
443 reaction would lead to the formation of $(CH_3)_2CHO$ radical (60%) and $CH_3C(O)CH_3$ +
444 $(CH_3)_2CHOH$ (40%). CH_3CH_2O and $(CH_3)_2CHO$ alkoxy radicals are expected to react
445 with O_2 to form HCHO, CH_3CHO and $CH_3C(O)CH_3$.

446

447 **3.4. Photolysis of perfluoro-3-methyl-2-butanone**

448 PF-3M2B/SF_6/air mixtures were monitored for 2 hours in the dark in HELIOS.
449 The dark loss rates of SF_6 and PF-3M2B were similar and found to be (1.1-1.3) $\times 10^{-5}$
450 s^{-1}. The gas mixture PF-3M2B /SF_6/air was exposed to solar irradiation for typically 5-
451 6 hours. PF-3M2B was monitored by FTIR and PTR-TOF-MS (CF_3^+ and $(CF_3)_2CF_3^+$
452 ions at *m/z* 68.986 and *m/z* 168.970, respectively). The observed loss of PF-3M2B
453 ranged from 1.3 to 2.0% depending on the solar light intensity. The obtained photolysis
454 rate was $J_{PF\text{-}3M2B} = (9\pm5)\times10^{-7}$ s^{-1} with $J_{NO2} = (4.2\text{-}7.7)\times10^{-3}$ s^{-1}. The experimental
455 conditions and the corresponding results are summarized in Table 1. The TUV model

was also used to calculate the PF-3M2B photolysis loss rates at the different period of year, ranging from 2×10^{-7} s^{-1} to 1.2×10^{-6} s^{-1}. No detectable formation of products was observed from the photolysis of PF-3M2B due to its low photolysis rate and to the detection limits of the analytical techniques used.

The maximum photolysis rate constant of PF-3M2B, $J_{max\text{-}PF\text{-}3M2B}$, was estimated using the integrated UV absorption spectrum over the actinic flux region and found to be $J_{max\text{-}PF\text{-}3M2B} = (2.9\text{-}5.6) \times 10^{-5}$ s^{-1}. The measured photolysis rate led to an effective photolysis quantum yield estimated to $\emptyset_{eff} \leq 0.037$ under tropospheric sunlight conditions.

3.5 Infrared absorption and global warming potential (GWP)

The infrared absorption spectra of the PF-2M3P and PF-3M2B measured in this work are characterized by broad diffuse vibrational bands as shown in Figure 3, (digitized absorption spectra are provided in SI as .txt format). The spectra are characterized by strong absorption features in the C-F stretch regions, 1200-1400 cm^{-1}. Overall, the larger perfluorinated ketones have greater peak cross sections in this region due, in part, to the greater overlap of vibrational bands. The infrared spectrum of 2M3P is also characterized by broad vibrational band, due to absorption features of C-H stretch regions. The IR spectrum of 2M3P is also characterized by a sharp absorption at 1700 cm^{-1}, corresponding to C=O stretch vibration (Figure 3). Corresponding graphical representations of Beer's law fits are given in Figures S12, S13 and S14.

The integrated band strengths over the 700-2000 cm^{-1} region were determined to be 3.68×10^{-16}, 3.03×10^{-16} and 1.0×10^{-16} cm^2 $molecule^{-1}$ cm^{-1} (base *e*) for PF-2M3P, PF-3M2B and 2M3P, respectively. Integrated band strengths of PF-2M3P over the 700-2000 cm^{-1} IR spectral region reported by Díaz-de-Mera, et al. [13] (3.94×10^{-16} cm^2 $molecule^{-1}$ cm^{-1}) and D'Anna, et al. [18] (4.05×10^{-16} cm^2 $molecule^{-1}$ cm^{-1}) are in agreement with the present results, within 7% and 9%, respectively. To the best of our knowledge, IR spectra of PF-3M2B and 2M3P are reported for the first time in this work.

The radiative efficiencies (RE) for the investigated ketones were calculated using the experimentally measured spectra and the method given in Hodnebrog, et al. [25]. The RE values obtained in this work are 0.357, 0.304 and 1.78×10^{-6} W m^{-2} $ppbv^{-1}$ for PF-2M3P, PF-3M2B and 2M3P, respectively for atmospherically well-mixed conditions and + 10% stratospheric temperature correction.

However, the radiative forcing for the present ketones is expected to be minor due to their expected short atmospheric lifetimes, < 13 days, and low atmospheric abundances. Therefore, lifetime-adjusted RE, accounting for non-uniform horizontal and vertical mixing for very short-lived compounds, was preferred and calculated to be 0.012-0.036, ~0.036 and $\leq 4 \times 10^{-8}$ W m^{-2} $ppbv^{-1}$ for PF-2M3P, PF-3M2B and 2M3P, respectively. Corresponding GWPs (for 100 years horizon) were found to be <0.21, ~0.29 and $\leqslant 1.3 \times 10^{-7}$ for PF-2M3P, PF-3M2B and 2M3P, respectively, showing a minor contribution of the studied ketones to the global warming potential. As shown in

Table S4, GWP of PF-2M3P is in good agreement with the studies of Díaz-de-Mera, et al. [13] and Hodnebrog, et al. [25].

4. Atmospheric implications

The photolysis rate of PF-2M3P was measured in September 2013 and July 2010 under natural irradiation and found to be (1.1-3.8) $\times 10^{-6}$ s^{-1} and (1.7-2.8) $\times 10^{-6}$ s^{-1}, respectively (J_{NO2} = (3.3-5.6)$\times 10^{-3}$ s^{-1}) leading to an atmospheric lifetime of PF-2M3P with respect to photolysis in the range of 3-11 days considering that the photolysis occurs during the daytime, which is in good agreement with the literature results, i.e., 4-14 days.[5-6, 13, 18] The hydrolysis as removal process was demonstrated to be too slow to be considered of atmospheric importance.[5-6] Besides, due to a high air-water partition coefficient,[26] very low quantities of PF-2M3P will be present in the cloud droplets. Based on the upper limits for the reaction rate coefficients (in units of cm^3 $molecule^{-1}$ s^{-1}) with OH radical ($<5 \times 10^{-16}$), O_3 ($<4 \times 10^{-22}$) and Cl atoms ($<1.7 \times 10^{-19}$) taken from Taniguchi, et al. [5] and typical global average tropospheric concentrations (in molecule cm^{-3}) of OH ~ 2×10^6,[27] Cl ~ 10^4,[28] and O_3 ~ 7×10^{11},[29] the tropospheric lifetime towards OH, Cl and O_3 reactions is equivalent to > 30 years. Thus, it is concluded that the photolysis will be the dominant atmospheric loss process for PF-2M3P.

Based on the photolysis rate measurement of PF-3M2B under natural irradiation ($J_{PF\text{-}3M2B}$ = (9±5)$\times 10^{-7}$ s^{-1}), an atmospheric lifetime with respect to photolysis of ~13 days was derived. To the best of our knowledge, this work provides the first photolysis

519 study of PF-3M2B. By analogy with PF-2M3P, other processes such as reactions with
520 OH radical, Cl and O_3 and hydrolysis would not contribute significantly to the
521 atmospheric removal of PF-3M2B.

522 Using the photolysis rates of 2M3P measured under natural irradiation (J_{2M3P} =
523 $\leq(2.6\pm1.4)\times10^{-6}$ s^{-1}), an atmospheric lifetime with respect to photolysis of ≥4 days was
524 derived. In addition to photolysis, gas phase reactions with OH radical and Cl atom
525 could also contribute significantly to the tropospheric loss of 2M3P. Indeed,
526 tropospheric lifetimes towards OH and Cl reactions were derived to be ≈ 4 (OH rate
527 coefficient estimated from SAR) [30] and 11 days [31], respectively. Thus, both photolysis
528 and gas phase loss processes will contribute to the loss of 2M3P in the troposphere.
529 Therefore, the tropospheric lifetime, τ_{tot}, defined as $\frac{1}{\tau_{tot}} = \frac{1}{\tau_{OH}}+\frac{1}{\tau_{Cl}}+\frac{1}{\tau_{hv}}$ with τ_{OH}, τ_{Cl}
530 and τ_{OH}, the corresponding lifetimes with respect to photolysis and OH radical and Cl
531 reactions, respectively, was estimated to be 1-2 days.

532 Based on the present study, the photolysis of PF-2M3P has been found to produce
533 $CF_3C(O)F$, COF_2, TFA, PFPrA, and CO under natural conditions. In the atmosphere,
534 $CF_3C(O)F$ will mainly hydrolyze to give trifluoroacetic acid (TFA, $CF_3C(O)OH$). In
535 the lower atmosphere, COF_2 will be lost through hydrolysis,[32-33] whereas in the
536 stratosphere, the photolysis is the dominant pathway producing CO_2 and HF,[34] leading
537 to a local lifetime of 5-10 days. [35]

538 The photolysis of 2M3P in the troposphere will lead to the formation of
539 $CH_3C(O)CH_3$, CH_3CHO, HCHO and CO. The major atmospheric loss of $CH_3C(O)CH_3$,

CH_3CHO and HCHO is controlled by photolysis and reaction with OH radical. Their photolysis are a source of HO_X (OH, HO_2) in the upper troposphere.[16,36]

Finally, the low GWP values and the short atmospheric lifetimes for the studied ketones may not lead to a large impact on the global warming of the Earth's atmosphere but may have some impact regarding the formation of other fluorinated species.

ASSOCIATED CONTENT

Supporting Information

UV absorption cross section of PF-2M3P, PF-3M2B and 2M3P are provided in Table S1 and Beer's law fits in Figure S2; UV absorption spectra of acetone is displayed in Figure S1; Seasonal dependence of the photolysis rate of PF-2M3P, PF-3M2B and 2M3P simulated using TUV Model is tabulated in Table S2; Figures S3 and S4 represents the FTIR spectra and GC-MS spectrum, respectively and were used to obtain the products yield as shown in Figures S5 and S6. Formation yields from the photolysis of PF-2M3P are summarized in Table S3. Corresponding photolysis pathway is proposed in Figure S7; Figure S8 presents the FTIR spectra from irradiation of 2M3P. Figure S10 presents the data used to derive the formation yield of products from the loss of 2M3P (Figure S9). Corresponding proposed photolysis pathway is given in Figure S11. Infrared absorption cross sections of 2M3P, PF-2M3P and PF-3M2B (.txt format) used to calculate radiative efficiencies (RE) and GWPs (100 years) (Table S4) and the fitting according to Beer's law (Figure S12, Figure 13 and Figure S14).

AUTHOR INFORMATION

Corresponding Author

*Tel: 33 (0)2 38 25 76 12; e-mail: mellouki@cnrs-orleans.fr.

ORCID

Yangang Ren: 0000-0001-5770-5050

François Bernard: 0000-0002-6116-3167

Véronique Daële: 0000-0003-2509-4077

Abdelwahid Mellouki: 0000-0002-6594-5262

Acknowledgments

574 This work is supported by Labex Voltaire (ANR-10-LABX-100-01), ARD PIVOTS
575 program (supported by the Centre-Val de Loire regional council), and the European
576 Union’s Horizon 2020 research and innovation programme through the
577 EUROCHAMP-2020 Infrastructure Activity under grant agreement No. 730997.
578

References

(1) Forrest, E. C.; Hu, L.-W.; Buongiorno, J.; McKrell, T. J., Pool Boiling Heat Transfer Performance of a Dielectric Fluid With Low Global Warming Potential. *Heat Transfer Eng.* **2013,** *34* (15), 1262-1277.

(2) Yao, B.; Vollmer, M. K.; Zhou, L. X.; Henne, S.; Reimann, S.; Li, P. C.; Wenger, A.; Hill, M., In-situ measurements of atmospheric hydrofluorocarbons (HFCs) and perfluorocarbons (PFCs) at the Shangdianzi regional background station, China. *Atmos. Chem. Phys.* **2012,** *12* (21), 10181-10193.

(3) Schaefer, D. O.; Godwin, D.; Harnisch, J., Estimating Future Emissions and Potential Reductions of HFCs, PFCs, and SF_6. *Energy J.* **2006,** *27*, 63-88.

(4) Hyrenbach, M. In *Alternative gas insulation in medium-voltage switchger*, 23rd International Conference on Electricity Distribution, Lyon, 15-18 June; Lyon, 2015.

(5) Taniguchi, N.; Wallington, T. J.; Hurley, M. D.; Guschin, A. G.; Molina, L. T.; Molina, M. J., Atmospheric Chemistry of $C_2F_5C(O)CF(CF_3)_2$: Photolysis and Reaction with Cl Atoms, OH Radicals, and Ozone. *J. Phys. Chem. A* **2003,** *107* (15), 2674-2679.

(6) Jackson, D. A.; Young, C. J.; Hurley, M. D.; Wallington, T. J.; Mabury, S. A., Atmospheric Degradation of Perfluoro-2-methyl-3-pentanone: Photolysis, Hydrolysis and Hydration. *Environ. Sci. Technol.* **2011,** *45* (19), 8030-8036.

(7) Hyrenbach, M.; Zache, S. In *Alternative insulation gas for medium-voltage switchgear*, 2016 Petroleum and Chemical Industry Conference Europe (PCIC Europe), 14-16 June 2016; 2016; pp 1-9.

(8) Mu, Y. J.; Mellouki, A., The near-UV absorption cross sections for several ketones. *J. Photochem. Photobiol., A* **2000,** *134* (1-2), 31-36.

(9) Ren, Y.; Grosselin, B.; Daele, V.; Mellouki, A., Investigation of the reaction of ozone with isoprene, methacrolein and methyl vinyl ketone using the HELIOS Chamber. *Faraday Discussions* **2017,** *200* (0), 289-311.

(10) Volkamer, R.; Platt, U.; Wirtz, K., Primary and Secondary Glyoxal Formation from Aromatics: Experimental Evidence for the Bicycloalkyl−Radical Pathway from Benzene, Toluene, and p-Xylene. *J. Phys. Chem. A* **2001,** *105* (33), 7865-7874.

(11) Atkinson, R.; Baulch, D. L.; Cox, R. A.; Crowley, J. N.; Hampson, R. F.; Hynes, R. G.; Jenkin, M. E.; Rossi, M. J.; Troe, J.; Subcommittee, I., Evaluated kinetic and photochemical data for atmospheric chemistry: Volume II – gas phase reactions of organic species. *Atmos. Chem. Phys.* **2006,** *6* (11), 3625-4055.

(12) J. B. Burkholder; S. P. Sander; J. Abbatt; J. R. Barker; R. E. Huie; C. E. Kolb; M. J. Kurylo; V. L. Orkin; D. M. Wilmouth; Wine, P. H., Chemical Kinetics and Photochemical Data for Use in Atmospheric Studies, Evaluation No. 18. JPL Publication 15-10, J. P. L., Ed. Pasadena,, 2015.

(13) Díaz-de-Mera, Y.; Aranda, A.; Notario, A.; Rodriguez, A.; Rodriguez, D.; Bravo, I., Photolysis study of fluorinated ketones under natural sunlight conditions. *Phys. Chem. Chem. Phys.* **2015,** *17* (35), 22991-22998.

(14) Yu, X.; Hou, H.; Wang, B., Atmospheric Chemistry of Perfluoro-3-methyl-2-butanone [CF3C(O)CF(CF3)2]: Photodissociation and Reaction with OH Radicals. *J. Phys. Chem. A* **2018,** *122* (45), 8840-8848.

(15) Chiappero, M. S.; Malanca, F. E.; Argüello, G. A.; Wooldridge, S. T.; Hurley, M. D.; Ball, J. C.; Wallington, T. J.; Waterland, R. L.; Buck, R. C., Atmospheric Chemistry of Perfluoroaldehydes ($C_xF_{2x+1}CHO$) and Fluorotelomer Aldehydes ($C_xF_{2x+1}CH_2CHO$): Quantification of the Important Role of Photolysis. *J. Phys. Chem. A* **2006,** *110* (43), 11944-11953.

(16) Simpson, W. R.; von Glasow, R.; Riedel, K.; Anderson, P.; Ariya, P.; Bottenheim, J.; Burrows, J.; Carpenter, L. J.; Frieß, U.; Goodsite, M. E.; Heard, D.; Hutterli, M.; Jacobi, H. W.; Kaleschke, L.; Neff, B.; Plane, J.; Platt, U.; Richter, A.; Roscoe, H.; Sander, R.; Shepson, P.; Sodeau, J.; Steffen, A.; Wagner, T.; Wolff, E., Halogens and their role in polar boundary-layer ozone depletion. *Atmos. Chem. Phys.* **2007,** *7* (16), 4375-4418.

(17) Metcalfe, J.; Phillips, D., Photophysical processes in fluorinated acetones. *J. Chem. Soc., Faraday Trans. 2,* **1976,** *72* (0), 1574-1583.

(18) D'Anna, B.; Sellevåg, S. R.; Wirtz, K.; Nielsen, C. J., Photolysis Study of Perfluoro-2-methyl-3-pentanone under Natural Sunlight Conditions. *Environ. Sci. Technol.* **2005,** *39* (22), 8708-8711.

(19) Madronich, S.; Flocke, S., The Role of Solar Radiation in Atmospheric Chemistry. In *Environmental Photochemistry*, Boule, P., Ed. Springer Berlin Heidelberg: Berlin, Heidelberg, 1999; pp 1-26.

(20) Sehested, J.; Ellermann, T.; Nielsen, O. J.; Wallington, T. J.; Hurley, M. D., UV Absorption Spectrum, and Kinetics and Mechanism of the Self Reaction of $CF_3CF_2O_2$ Radicals in the Gas Phase at 295 K. *Int. J. Chem. Kinet.* **1993,** *25* (9), 701-717.

(21) Wallington, T. J.; Hurley, M. D.; Schneider, W. F.; Sehested, J.; Nielsen, O. J., Atmospheric chemistry of trifluoromethoxy radicals: reaction with water. *J. Phys. Chem.* **1993,** *97* (29), 7606-7611.

(22) Young, C. J.; Donaldson, D. J., Overtone-Induced Degradation of Perfluorinated Alcohols in the Atmosphere. *J. Phys. Chem. A* **2007,** *111* (51), 13466-13471.

(23) Le Crâne, J.-P.; Villenave, E.; Hurley, M. D.; Wallington, T. J.; Ball, J. C., Atmospheric Chemistry of Propionaldehyde: Kinetics and Mechanisms of Reactions with OH Radicals and Cl Atoms, UV Spectrum, and Self-Reaction Kinetics of $CH_3CH_2C(O)O_2$ Radicals at 298 K. *J. Phys. Chem. A* **2005,** *109* (51), 11837-11850.

(24) Lightfoot, P. D.; Cox, R. A.; Crowley, J. N.; Destriau, M.; Hayman, G. D.; Jenkin, M. E.; Moortgat, G. K.; Zabel, F., Organic peroxy-radicals-kinetics, spectroscopy and tropospheric chemistry. *Atmos. Environ.* **1992,** *26* (10), 1805-1961.

(25) Hodnebrog, Ø.; Etminan, M.; Fuglestvedt, J. S.; Marston, G.; Myhre, G.; Nielsen, C. J.; Shine, K. P.; Wallington, T. J., Global warming potentials and radiative efficiencies of halocarbons and related compounds: A comprehensive review. *Rev. Geophys.* **2013,** *51* (2), 300-378.

(26) Rayne, S.; Forest, K., Prediction of the air-water partition coefficient for perfluoro-2-methyl-3-pentanone using high-level Gaussian-4 composite theoretical methods. *J. Environ. Sci. Health., Part A* **2014,** *49* (11), 1228-1235.

(27) Hein, R.; Crutzen, P. J.; Heimann, M., An inverse modeling approach to investigate the global atmospheric methane cycle. *Global Biogeochem. Cycles* **1997,** *11* (1), 43-76.

(28) Saiz-Lopez, A.; von Glasow, R., Reactive halogen chemistry in the troposphere. *Chem. Soc. Rev.* **2012,** *41* (19), 6448-6472.

(29) Monks, P. S.; Granier, C.; Fuzzi, S.; Stohl, A.; Williams, M. L.; Akimoto, H.; Amann, M.; Baklanov, A.; Baltensperger, U.; Bey, I.; Blake, N.; Blake, R. S.; Carslaw, K.; Cooper, O. R.; Dentener, F.; Fowler, D.; Fragkou, E.; Frost, G. J.; Generoso, S.; Ginoux, P.; Grewe, V.; Guenther, A.; Hansson, H. C.; Henne, S.; Hjorth, J.; Hofzumahaus, A.; Huntrieser, H.; Isaksen, I. S. A.; Jenkin, M. E.; Kaiser, J.; Kanakidou, M.; Klimont, Z.; Kulmala, M.; Laj, P.; Lawrence, M. G.; Lee, J. D.; Liousse, C.; Maione, M.; McFiggans, G.; Metzger, A.; Mieville, A.; Moussiopoulos, N.; Orlando, J. J.; O'Dowd, C. D.; Palmer, P. I.; Parrish, D. D.; Petzold, A.; Platt, U.; Pöschl, U.; Prévôt, A. S. H.; Reeves, C. E.; Reimann, S.; Rudich, Y.; Sellegri, K.; Steinbrecher, R.; Simpson, D.; ten Brink, H.; Theloke, J.; van der Werf, G. R.; Vautard, R.; Vestreng, V.; Vlachokostas, C.; von Glasow, R., Atmospheric composition change – global and regional air quality. *Atmos. Environ.* **2009,** *43* (33), 5268-5350.

(30) Kwok, E. S. C.; Atkinson, R., Estimation of hydroxyl radical reaction rate constants for gas-phase organic compounds using a structure-reactivity relationship: An update. *Atmos. Environ.* **1995,** *29* (14), 1685-1695.

(31) Ren, Y.; Wang, J.; Grosselin, B.; Daële, V.; Mellouki, A., Kinetic and product studies of Cl atoms reactions with a series of branched Ketones. *J. Environ. Sci.* **2018,** *71*, 271-282.

(32) Houde, M.; Martin, J. W.; Letcher, R. J.; Solomon, K. R.; Muir, D. C. G., Biological Monitoring of Polyfluoroalkyl Substances: A Review. *Environ. Sci. Technol.* **2006,** *40* (11), 3463-3473.

(33) Hanson, D. R.; Ravishankara, A. R., The loss of CF_2O on Ice, Nat, and Sulfuric-acid-solutions. *Geophys. Res. Lett.* **1991,** *18* (9), 1699-1701.

(34) Nolle, A.; Krumscheid, C.; Heydtmann, H., Determination of quantum yields in the UV photolysis of COF_2 and COFCl. *Chem. Phys. Lett.* **1999,** *299* (6), 561-565.

(35) WMO (World Meteorological Organization) *Scientific Assessment of Ozone Depletion: 2010, Global Ozone Research and Monitoring Project–Report*; Switzerland, Geneva, 2011; p 516

(36) Jaegle, L.; Jacob, D. J.; Brune, W. H.; Wennberg, P. O., Chemistry of HO_x radicals in the upper troposphere. *Atmos. Environ.* **2001,** *35* (3), 469-489.

Table 1. Experimental conditions and obtained results for the photolysis of perfluoro-2-methyl-3-pentanone (PF-2M3P), perfluoro-3-methyl-2-butanone (PF-3M2B) and 2-methyl-3-pentanone (2M3P).

	[ketone]	J_{NO2}	Photolysis loss	Irradiation period	J (10^{-6} s^{-1})		
	(10^{13} molecule cm^{-3})	(10^{-3} s^{-1})	(%)	(h:mm)	FT-IR	GC-MS[b]/ PTR-TOF-MS[c]	Rec [a]
	3.4 m^3 outdoor chamber						
PF-2M3P	18	4.4±1.1	3.7	4:23	2.3±0.2	-	2.3±0.4
	18	4.9±0.9	3.7	4:18	2.8±0.2	-	2.8±0.4
	27	4.4±1.5	2.1	3:39	1.7±0.2	-	1.7±0.4
	8.9	5.5±0.6	2.8	4:13	1.9±0.3	-	1.9±0.6
	HELIOS						
	3.8	3.0±0.4	1.7	4:32	1.1±0.1	1.1±0.1[b]	1.1±0.4
	3.0	5.3±1.0	7.7	5:01	3.8±0.3	3.5±0.5[b]	3.8±1.0
	3.6	4.6±1.2	6.1	7:11	2.2±0.3	2.3±0.4[b]	2.2±0.8
	3.5	5.6±0.7	7.4	7:08	3.7±0.5	3.6±0.5[b]	3.6±1.0
2M3P	3.3	2.9±1.2	5.7	6:00	1.6±0.7	1.5±0.4[b]	1.6±1.0
	3.4	2.2±0.3	3.9	5:49	1.2±0.2	1.3±0.4[b]	1.2±0.8
	3.4	2.4±1.1	3.9	6:14	1.5±0.2	1.7±0.3[b]	1.6±0.6
	3.3	5.6±0.5	6.3	5:26	2.7±0.7	2.6±0.7[b]	2.6±1.4
	3.4	5.1±0.5	5.3	6:01	2.1±0.7	2.0±0.4[b]	2.0±1.0
	3.4	5.1±0.7	4.8	4:58	2.0±0.6	2.0±0.4[b]	2.0±1.2
PF-3M2B	0.09	7.6±1.3	< 0.2%	5:30	< 1%	-	
	0.05	7.7±1.4	< 0.2%	5:17	< 1%	-	
	1.5	4.2±1.8	2.0	5:07	1.1	-	1.1
	4.2	5.8±1.1	1.3	5:30	0.67	0.28[c]	0.48±0.28
	3.9	6.3±1.4	1.7	6:08	0.8	1.2[c]	0.98±0.50

[a] Recommended value obtained from the weighted average of each individual measurement: $J_{av}=(w_1J_1+ w_2J_2 + \ldots)/(w_1+ w_2+\ldots)$, where $w=1/\sigma^2$, etc. The error, is given by: $2\sigma_{av}=(\sigma_1^2+\sigma_2^2+ \ldots)^{0.5}$

[b] measured using GC-MS

[c] measured using PTR-TOF-MS

Table 2. Photolysis rate of perfluoro-2-methyl-3-pentanone (PF-2M3P), perfluoro-3-methyl-2-butanone (PF-3M2B) and 2-methyl-3-pentanone (2M3P) obtained in this work and compared to the reported data from the literature.

Ketone	$[Ketone]_0$ (10^{13} molecule cm^{-3})	Chamber	Date	Irradiation	J (s^{-1})	J_{NO2} (s^{-1})	Atmospheric Lifetime (days)	Reference
PF-2M3P	3.0-3.8	HELIOS	Sept 2013	Solar irradiation	$(1.1\text{-}3.8)\times10^{-6}$	$(3.0\text{-}5.6)\times10^{-3}$	3-11	This work
	8.9-27	3.4 m^3 chamber	July 2010	Solar irradiation	$(1.7\text{-}2.8)\times10^{-6}$	$(4.4\text{-}5.5)\times10^{-3}$	4-7	This work
	8-64	Toledo, Spain	June-July 2013/2014	Solar irradiation	$(6.8\pm0.8)\times10^{-6}$		5.5±1.9	Díaz-de-Mera, et al. [13]
	2.5	Euphore	July 2003	Solar irradiation	$(6.4\pm0.3)\times10^{-6}$	7.85×10^{-3}	~7	D'Anna, et al. [18]
	$(0.55\text{-}6.5)\times10^{3}$	140-L Pyrex reactor		14 blacklamps 8 sunlamps	$(1.0\pm0.1)\times10^{-7}$ $(6\pm2)\times10^{-7}$		7-14	Taniguchi, et al. [5]
	47° N and 1° E[a]		a	TUV model	$(0.4\text{-}2.8)\times10^{-6}$			This work
	39.9° N and 4° W[a]		a	TUV model	$(2.1\pm0.8)\times10^{-6}$		5.5±1.9	Díaz-de-Mera, et al. [13]
	Different latitude[a]		a	TUV model	$(0.82\text{-}3.1)\times10^{-6}$		4-14	Jackson, et al. [6]
2M3P	3.0-3.4	HELIOS	Oct 2013	Solar irradiation	$\leq(2.6\pm1.4)\times10^{-6}$	$(2.2\text{-}5.6)\times10^{-3}$	1-2	This work
	47° N and 1° E[a]		a	TUV model	$(0.3\text{-}2.8)\times10^{-6}$			This work
PF-3M2B	3.0-3.4	HELIOS	July 2017	Solar irradiation	$(9\pm5)\times10^{-7}$	$(4.2\text{-}7.7)\times10^{-3}$	~13	This work
	47° N and 1° E[a]		a	TUV model	$(0.2\text{-}1.2)\times10^{-6}$			This work

[a] yearly average;

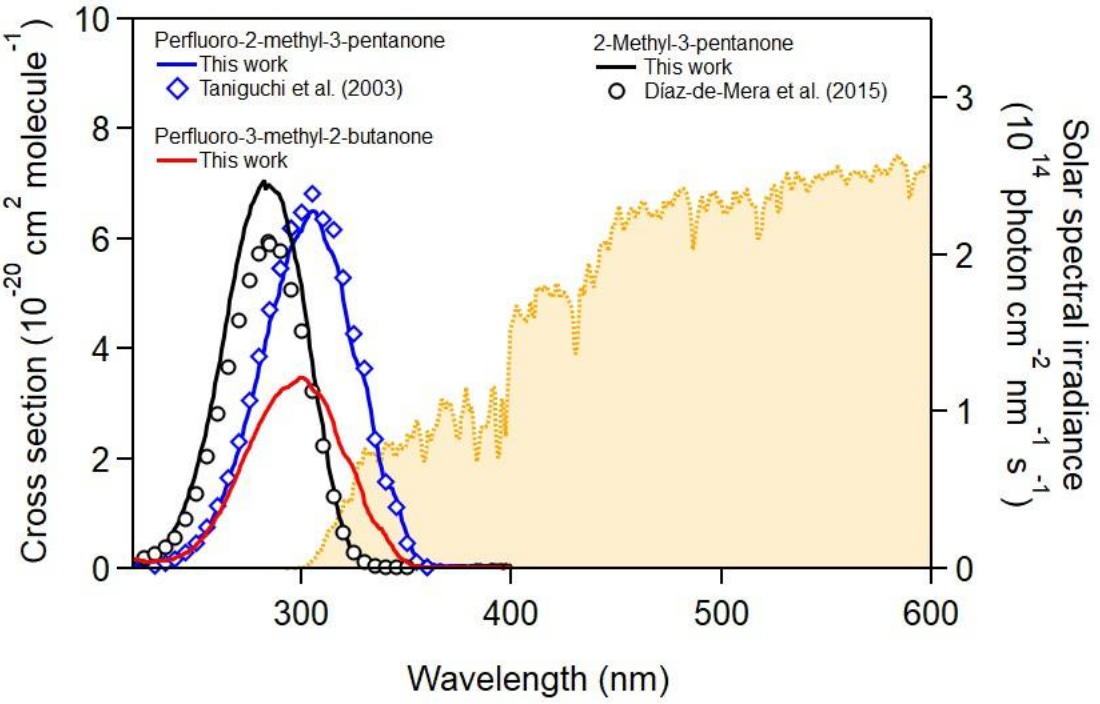
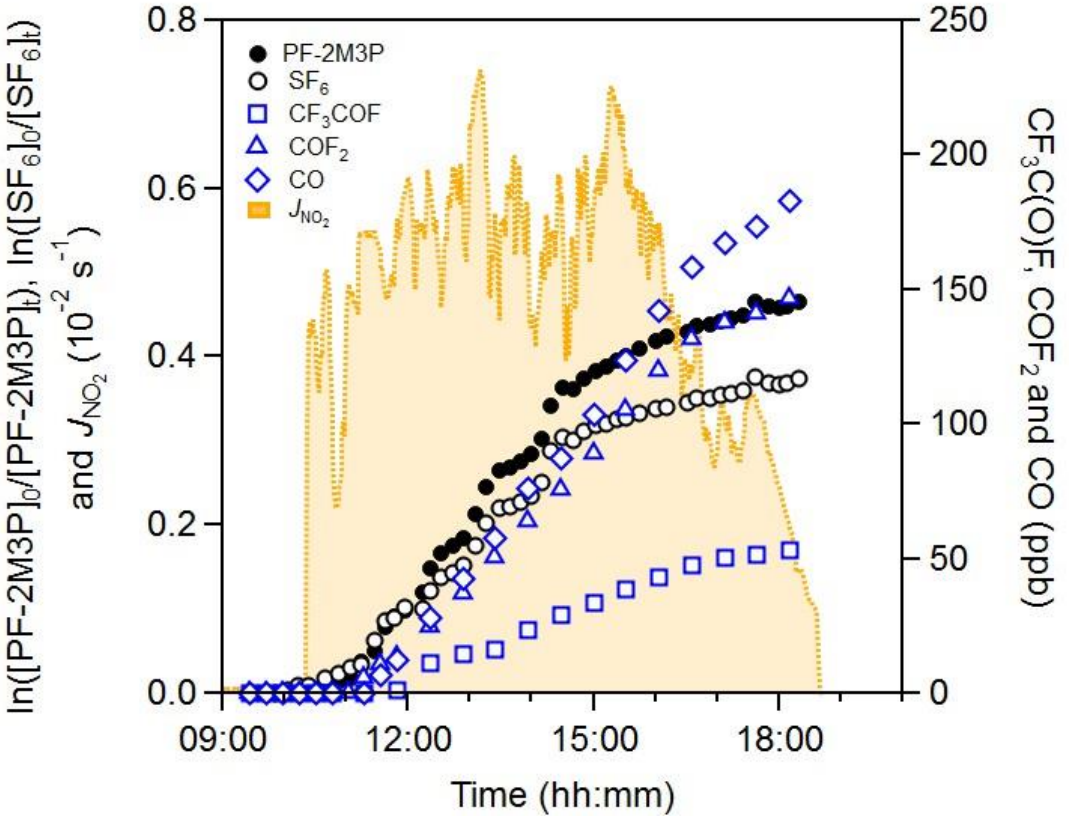


Figure 1. UV absorption spectra of perfluoro-2-methyl-3-pentanone (PF-2M3P), perfluoro-3-methyl-2-butanone (PF-3M2B) and 2-methyl-3-pentanone (2M3P) and compared with those from literature. The shaded area in yellow represents the solar spectral irradiance measured inside HELIOS (13:00 local time, 27 September 2013).

The figure 1 has been replaced

723



724

725 **Figure 2.** Perfluoro-2-methyl-3-pentanone (PF−2M3P) and its products during the
726 photolysis experiment under natural irradiation in HELIOS (27 September 2013).

727

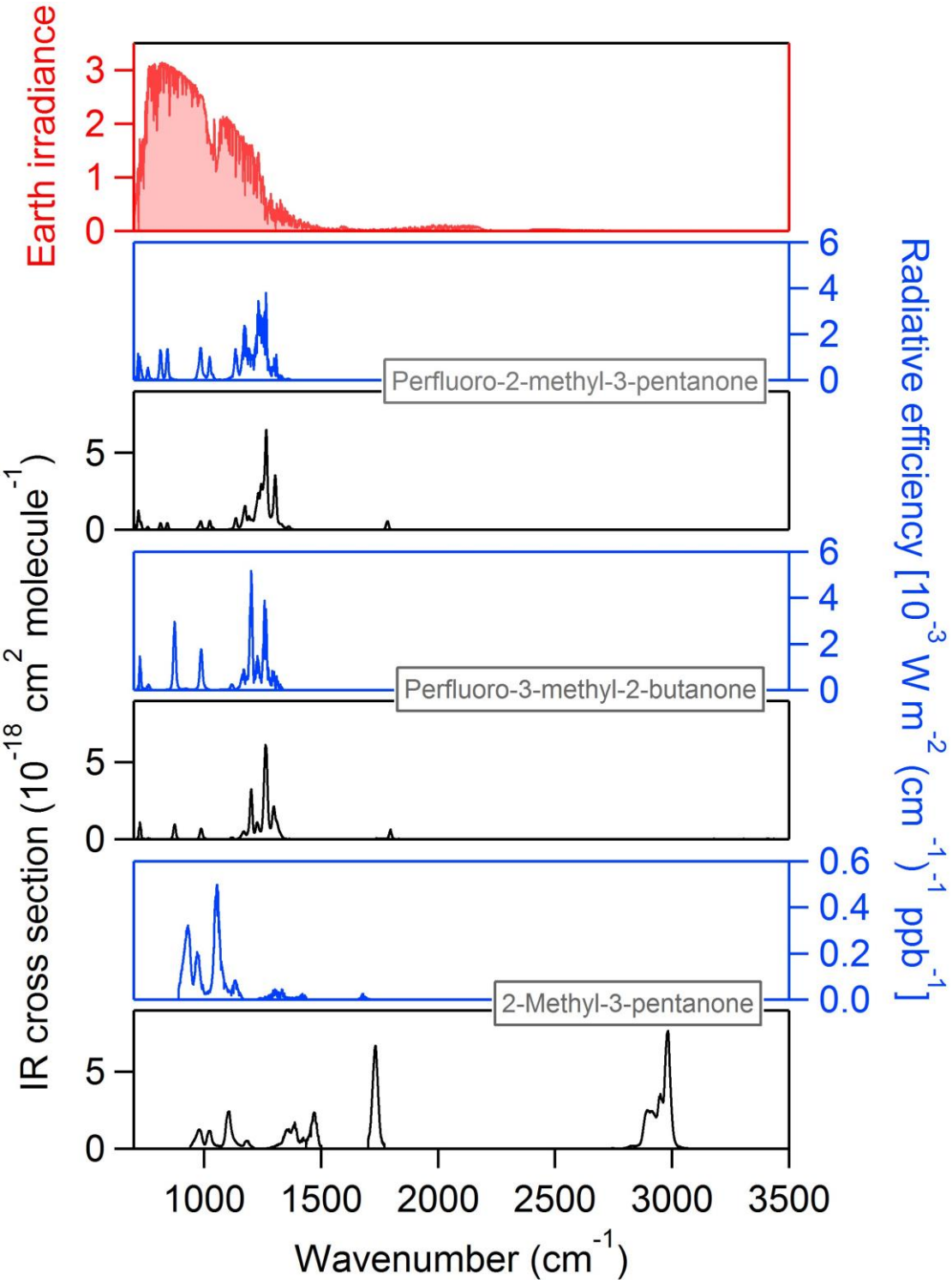


Figure 3. Infrared absorption of perfluoro-2-methyl-3-pentanone, perfluoro-3-methyl-2-butanone and 2-methyl-3-pentanone and their contributions to the radiative efficiency. Earth's irradiance spectrum (top panel) is reported by Hodnebrog, et al. [25] (in units of 10^{-3} W m^{-2} (cm^{-1})$^{-1}$ ppb^{-1} (10^{-18} cm^2 molecule^{-1})$^{-1}$). The infrared absorption spectra measured in this work are showed in black, lower panel (in units of 10^{-18} cm^2 molecule^{-1}, base e) and the radiative efficiency spectra are displayed in blue, upper panel (in units of W m^{-2} (cm^{-1})$^{-1}$ ppb^{-1}).